ISSN 1674-1056
http://cpb.iphy.ac.cn
http://iopscience.iop.org/cpb
中国物理 B
Chinese Physics
中国物理 Chinese Physics B

Field-variable magnetic domain characterization of individual 10 nm sized Fe_3O_4 nanoparticles

Zheng-Hua Li(李正华), Xiang Li(李翔), Wei Lu(陆伟)

Citation: Chin. Phys. B . 2019, 28(7): 077504. **doi:** 10.1088/1674-1056/28/7/077504
Journal homepage: http://cpb.iphy.ac.cn; http://iopscience.iop.org/cpb

What follows is a list of articles you may be interested in

Micromagnetic simulations of reversal magnetization in cerium-containing magnets

Lei Li(李磊), Shengzhi Dong(董生智), Hongsheng Chen(陈红升), Ruijiao Jiang(姜瑞姣), Dong Li(李栋), Rui Han(韩瑞), Dong Zhou(周栋), Minggang Zhu(朱明刚), Wei Li(李卫), Wei Sun(孙威)

Chin. Phys. B . 2019, 28(3): 037502. **doi:** 10.1088/1674-1056/28/3/037502

Magnetic properties of $L1_0$ FePt thin film influenced byrecoverable strains stemmed from the polarization of $Pb(Mg_{1/3}Nb_{2/3})O_3$-$PbTiO_3$ substrate

Li-Wang Liu(刘立旺), Cheng-Chao Hu(胡成超), Ye-Chuan Xu(徐野川), Hou-Bing Huang(黄厚兵), Jiang-Wei Cao(曹江伟), Linyun Liang(梁林云), Wei-Feng Rao(饶伟锋)

Chin. Phys. B . 2018, 27(7): 077503. **doi:** 10.1088/1674-1056/27/7/077503

Modeling of the loading path dependent magnetomechanical behavior of Galfenol alloy

Hui Jiang(江慧), Jie Zhu(朱洁)

Chin. Phys. B . 2017, 26(3): 037503. **doi:** 10.1088/1674-1056/26/3/037503

$L1_0$ FePt thin films with [001] crystalline growth fabricated by ZnO addition and rapid thermal annealing

Liu Xi, Ishio Shunji

Chin. Phys. B . 2013, 22(8): 087504. **doi:** 10.1088/1674-1056/22/8/087504

Composition influence on the microstructures and magnetic properties of FePt thin films

Liu Li-Wang, Dang Hong-Gang, Sheng Wei, Wang Ying, Cao Jiang-Wei, Bai Jian-Min, Wei FuLin

Chin. Phys. B . 2013, 22(4): 047503. **doi:** 10.1088/1674-1056/22/4/047503

Field-variable magnetic domain characterization of individual 10 nm Fe_3O_4 nanoparticles*

Zheng-Hua Li(李正华)[1], Xiang Li(李翔)[2,†], and Wei Lu(陆伟)[3]

[1] School of Physics and Materials Engineering, Dalian Minzu University, Dalian 116600, China
[2] School of Materials Science and Engineering, University of Shanghai for Science and Technology, Shanghai 200093, China
[3] School of Materials Science and Engineering, Tongji University, Shanghai 200092, China

(Received 25 January 2019; revised manuscript received 5 May 2019; published online 12 June 2019)

The local detection of magnetic domains of isolated 10 nm Fe_3O_4 magnetic nanoparticles (MNPs) has been achieved by field-variable magnetic force microscopy (MFM) with high spatial resolution. The domain configuration of an individual MNP shows a typical dipolar response. The magnetization reversal of MNP domains is governed by a coherent rotation mechanism, which is consistent with the theoretical results given by micromagnetic calculations. Present results suggest that the field-variable MFM has great potential in providing nanoscale magnetic information on magnetic nanostructures, such as nanoparticles, nanodots, skyrmions, and vortices, with high spatial resolution. This is crucial for the development and application of magnetic nanostructures and devices.

Keywords: Fe_3O_4 nanoparticles, magnetic force microscopy, magnetic domain

PACS: 75.50.Ss, 75.78.Cd **DOI:** 10.1088/1674-1056/28/7/077504

1. Introduction

Over the past few decades, the magnetic properties of iron oxide nanoparticles have been widely explored mainly due to their potential applications in various fields, including storage media, environmental remediation, and bio-medicine.[1–10] For scientific research, a precise characterization of the magnetic properties of individual magnetic nanoparticles (MNPs) is essential. In the last decade, the introduction of new experimental techniques, such as the anomalous Hall-effect,[11] superconducting quantum interference device,[12,13] spin-polarized scanning tunneling microscopy,[14] transmission x-ray microscopy,[15] and nitrogen-vacancy magnetometer[16], have helped us to obtain insight into the magnetic properties of individual and isolated MNPs. However, these techniques require a highly complex experimental apparatus and a dedicated sample preparation process. Although a lot of magnetic microscopy techniques have been developed over the past decades, imaging magnetism at a sub-10 nm nanoscale remains a challenging task because it requires a combination of high spatial resolution and sensitivity.[17]

Another remarkable technique that allows the direct imaging of magnetic nanostructures is magnetic force microscopy (MFM). It is an ideal tool to investigate the magnetic behaviors of nanosized magnets due to its high lateral resolution, which can provide microscopic information about the magnetic behavior of an individual nanomagnet.[18–26] The ability of MFM to detect superparamagnetic and low-coercivity MNPs, and the interpretation of the resulting MFM images, are subjects of ongoing research. Agarwal[22] reported the use of MFM to detect superparamagnetic nanoparticles (SPNs) with a dextran shell (giving a final diameter of 30–50 nm) in ambient atmospheric conditions. Sievers described the quantitative characterization of the magnetization of individual MNPs (about 19 nm in diameter) using MFM.[23] Park investigated the magnetic interactions of aggregated MNPs with a size of approximately 20–30 nm by using MFM with a Ferritin-based MFM probe.[24] Recently, Moya reported on the experimental characterization of the magnetic domain configurations in cubic isolated $Fe_{3-x}O_4$ nanoparticles with a lateral size of 25–30 nm.[25] Although successful attempts to characterize individual MNPs have been made,[22–26] the capability of MFM to detect a signal from nanoscale superparamagnetic particles with a grain size less than 10 nm has not been fully explored. A systematic study of the applicability of MFM for characterizing SPNs with a grain size less than 10 nm in ambient air is still lacking.

In addition, extensive experiments and theoretical studies show that the magnetization reversal process of MNPs is very complicated, and sometimes the results of these studies are not consistent with each other.[27–29] For instance, in some cases, the accurate value of reversal fields of MNPs was different from the value measured by conventional magnetometer instruments, or showed a different dependence on the diameters. Furthermore, when the nanoparticles become more and more dense, the magnetization reversal processes become affected by interparticle interactions.[30] On this basis, it is paramount

*Project supported by the National Natural Science Foundation of China (Grant Nos. 61771092 and 51202146) and the Natural Science Foundation of Shanghai, China (Grant No. 17ZR1419700).

†Corresponding author. E-mail: xiangli@usst.edu.cn

© 2019 Chinese Physical Society and IOP Publishing Ltd

to study the magnetization properties of individual nanoparticles as well as their mutual interactions.

In previous studies, we successfully carried out a direct imaging of magnetic domains and quantitative measurements of the magnetic information from individual superparamagnetic Fe_3O_4 nanoparticles by using MFM.[3,4] In this work, in order to better understand the magnetization reversal process of 10 nm-sized Fe_3O_4 MNPs, the frequency-modulated MFM[31] with a variable applied magnetic field is adopted to investigate the dynamic magnetization behavior of the Fe_3O_4 nanoparticles. A vibrating sample magnetometer is employed to measure the hysteresis loops of the Fe_3O_4 nanoparticles at room temperature to study the coercive field (H_c) and saturation magnetization (M_s) under a maximum magnetic field of $\pm$10 kOe. In addition, micromagnetic calculations are important for interpreting the experimental MFM images and providing some insight into the phenomenon taking place during the magnetization reversal of the Fe_3O_4 nanoparticles.

2. Experiments

The frequency modulation detection method is used in the field-variable MFM technique. Figure 1(a) shows the schematic diagram of the MFM system with a variable magnetic field. The ferrite core generates a homogeneous alternating magnetic field at the sample surface with an amplitude from -12 Oe to 12 Oe. A detailed description of the frequency-modulated MFM system has been given in Ref. [31]. It is possible to perform the measurement of the magnetic field gradient for the magnetic samples. Here, the sign (upward and downward) of the magnetic field reflects the polarity (N or S pole) of the surface magnetic pole. Thus, it is possible to directly detect the sign of the magnetic field to reflect the polarity of the surface magnetic pole of the magnetic samples.

The experiment was done in air atmosphere. The resonant frequency of the cantilever was about 256 kHz, and the Q value was about 500. The Fe_3O_4 MNPs were randomly distributed on the silicon substrate. After that, a thin layer (about 3 nm) of gold particles was sputtered on the MNPs, which were then covered and immobilized on the substrate, as shown in Fig. 1(b). The gold particles were obtained by using an ion sputter coater of a scanning electron microscope. The sputtering power, air pressure, and sputtering time were held at 15 W, 3 Pa, and 12 s, respectively. Tapping and lift mode AFM/MFM scans were carried out using a high-coercivity FePt tip ($H_c > 5$ kOe), which was coated with a thin FePt film with a radius of 10 nm. The lift height (tip-sample distance) was kept at 5–10 nm. The magnetization direction of the tip (which was magnetized before use) was perpendicular to the sample surface.

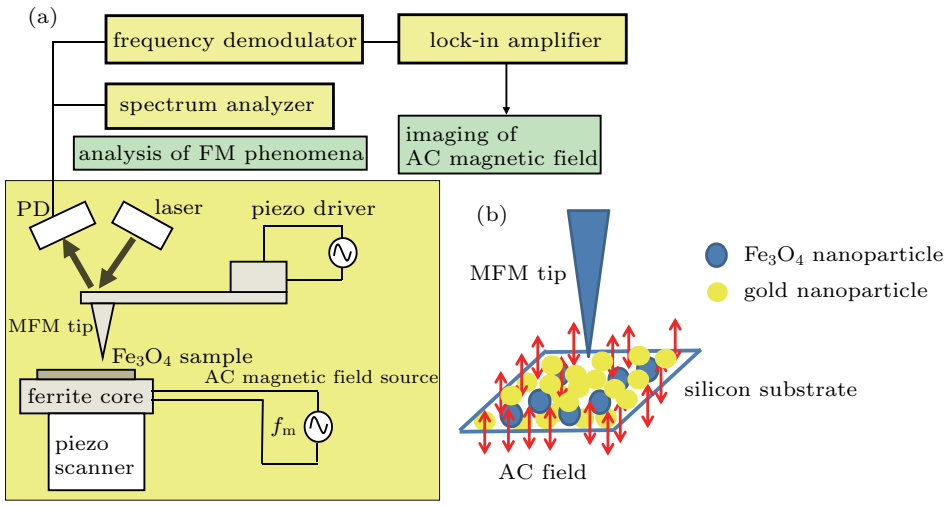


Fig. 1. Schematic diagrams of (a) the frequency-modulated MFM system and (b) sample status.

3. Results and discussion

Figure 2(a) shows the transmission electron microscopy (TEM) image of the as-synthesized Fe_3O_4 nanoparticles. The TEM image indicates the presence of small Fe_3O_4 particles of nanometric size. The diameters of most nanoparticles are within 20 nm, with the minority less than 10 nm, and some overlapping. Figure 2(b) shows the magnetic hysteresis loop of the Fe_3O_4 nanoparticles. The hysteresis loop shows that the as-synthesized Fe_3O_4 nanoparticles exhibit a saturation magnetization of $\sim$ 60 emu/g, which is in accordance with that of iron oxide nanoparticles with a similar size (typically in range of 40–70 emu/g). A magnification of the field range where these interceptions take place is shown in the inset of Fig. 2(b). The obtained coercive fields are about 6.8 Oe. This very small value of H_c for the studied MNPs suggests that the majority of the particles in this sample are superparamagnetic at room temperature.

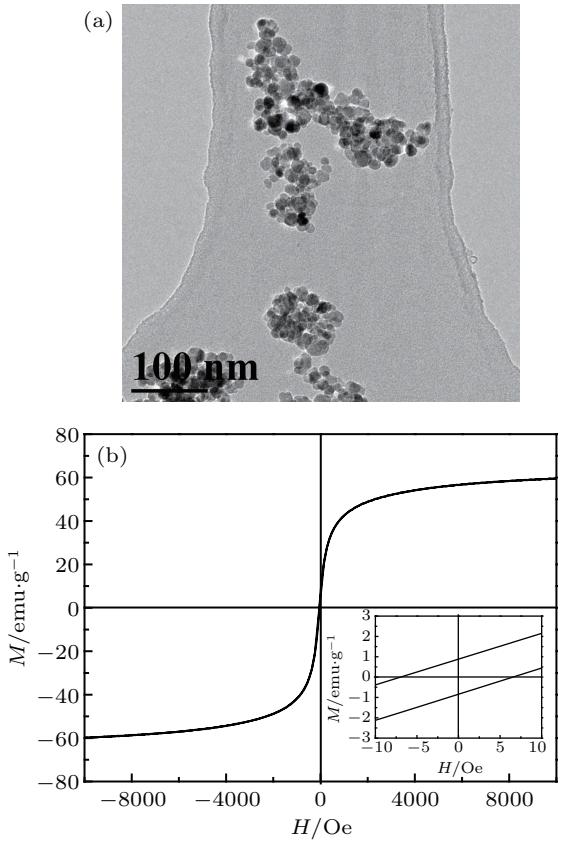


Fig. 2. (a) The TEM image of the as-synthesized Fe_3O_4 nanoparticles. (b) Magnetic hysteresis loop of the Fe_3O_4 nanoparticles (inset: zoom-in of the low-field region).

In Figs. 3(a) and 3(b), we give an example of the AFM/MFM images of the Fe_3O_4 nanoparticles without an external applied magnetic field (corresponding to the magnetic fields of 0 Oe). It can be seen that the topography (Fig. 3(a)) and phase (Fig. 3(b)) images are indeed well separated. The results show that the investigated surface has perfectly particle-like features, which presents the surface information of the uniform-sized gold particles. However, the magnetic signals observed from the MFM phase image are very weak (dark MFM contrasts, with a lift height of 5 nm), indicating a weak attractive force between the MFM tip and SPNs.

Figures 3(c)–3(h) show the field-variable MFM images of the Fe_3O_4 nanoparticles with the in-plane driven magnetic field H ranging from −10 Oe to 10 Oe in order to gain deeper insight into the magnetic nature of these isolated particles. As the external field varies, we observe no change in the topographic images but only in the magnetic phase images, thus confirming that the topographic images are not appreciably affected by the applied magnetic field. In the MFM images, almost all of the MNPs present a characteristic with bright–dark dipolar contrast. The bright area and dark area indicate a phase difference of $\sim 180°$. It is obvious that the magnetic particles remain distinguishable from the background. Moreover, it can be found that the magnetic contrast of the Fe_3O_4 MNPs changes uniformly with the applied magnetic fields. Similar magnetic domain structures with opposite polarities are seen when comparing MFM images at opposite values of the applied magnetic field. The MNPs show a typical dipolar contrast (bright and dark) after the application of various external magnetic fields, thus providing support for the single-domain structure in the samples. Considering that the individual particles are of superparamagnetism at zero field, the observed changes in magnetic polarization can be understood as just being induced by the action of the variable external magnetic field.

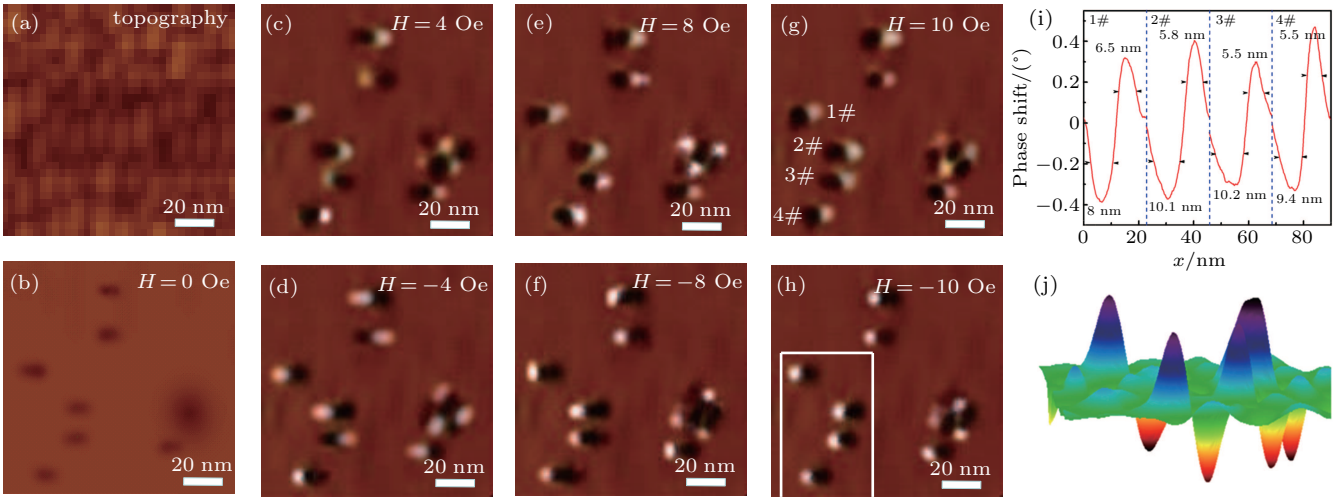


Fig. 3. MFM images in the same area of Fe_3O_4 samples. (a) Topography, (b)–(h) phase images with the various applied magnetic fields, (i) spectrum line profiles of particles 1#–4# shown in (g), and (j) 3-dimensional MFM image of the white line box area shown in (h).

Figure 3(i) shows the MFM signal profiles across the center of the selected nanoparticles (1#–4#) in Fig. 3(g). The spatial resolution of the MFM measurement in the current study is estimated from the spectrum line profiles of the MFM phase signals. The resolution is determined as the full width at half maximum of the peak signals. As shown in Fig. 3(i), the deter-

mined resolution is around 7.6 nm under the ambient condition with a lift height of 10 nm. Figure 3(j) clearly reveals the fine magnetic domain configurations of the individual MNPs corresponding to the four isolated nanoparticles with typical domain structures in the white line box of Fig. 3(h). The results imply that the four nanoparticles are all in a single domain state with a domain size of about 22 nm (estimated from the line profile), which is larger than the result determined from TEM experiments ($\sim$ 12 nm). This mainly resulted from the magnetic stray field at the boundary of MNPs. For all the magnetic domains of nanoparticles, left is bright (repulsive force), while right is dark (attractive force). This domain configuration is a typical dipolar response and can be considered as an in-plane magnetic domain. Summing up the magnetic properties of the Fe_3O_4 nanoparticles, we can conclude that they can be described as consisting of single-domain particles. The above results reveal that a stable magnetic dipole can be induced in SPNs by an external magnetic field of a few Oe at room temperature. Our MFM experiments reveal that the presence of an external magnetic field and a magnetic probe is essential to detect and distinguish the MFM signal from the SPNs. By applying a magnetic field to the sample, we could detect the in-plane dipole moment of SPNs as a combination of positive and negative phase contrasts. The field-dependent magnetic domains of the dipole moment in individual MNPs help confirm the presence of magnetic interaction between the MFM probe and the nanoparticles and also distinguish it from nonmagnetic contaminants present on the surface.

The recorded reversal of the spin configuration from one direction (for negative fields) to another one (for positive fields) is experimental evidence of the switching process being performed by a coherent rotation mechanism. In order to verify this presumption, micromagnetic calculations are performed to simulate the magnetization distribution in the Fe_3O_4 MNPs. In micromagnetic modeling, the total energies in each grid include the Zeeman energy, crystalline anisotropy energy, shape anisotropy energy, exchange interaction, and magnetostatic interaction. The simulation parameters are selected as follows: a saturation magnetization of 311 emu/cm^3 (at room temperature), and a magnetocrystalline anisotropy constant of 5.0×10^6 ergs/cm^3. The calculation of the magnetization reversals is accomplished based on the Landau–Lifshitz–Gilbert equation. The simulated MFM images are obtained by working out the first-order derivative of the magnetic field ($\partial H_z/\partial z$) at the sample surface.

The calculated in-plane hysteresis loop of a single MNP (10 nm) is shown in Fig. 4. This curve represents the magnetization reversal of the nanoparticle. The calculation suggests that the reversal mechanism of an individual Fe_3O_4 nanoparticle follows a coherent rotation of the spins, as indicated in Figs. 4(a)–4(c). Since the Fe_3O_4 nanoparticle is very small, the exchange energy may lead to the reversal process. The micromagnetic calculations suggest that a coherent rotation mechanism should be correlated with the magnetization reversal process observed in the MFM images, rather than with the nucleation and propagation of domain walls.

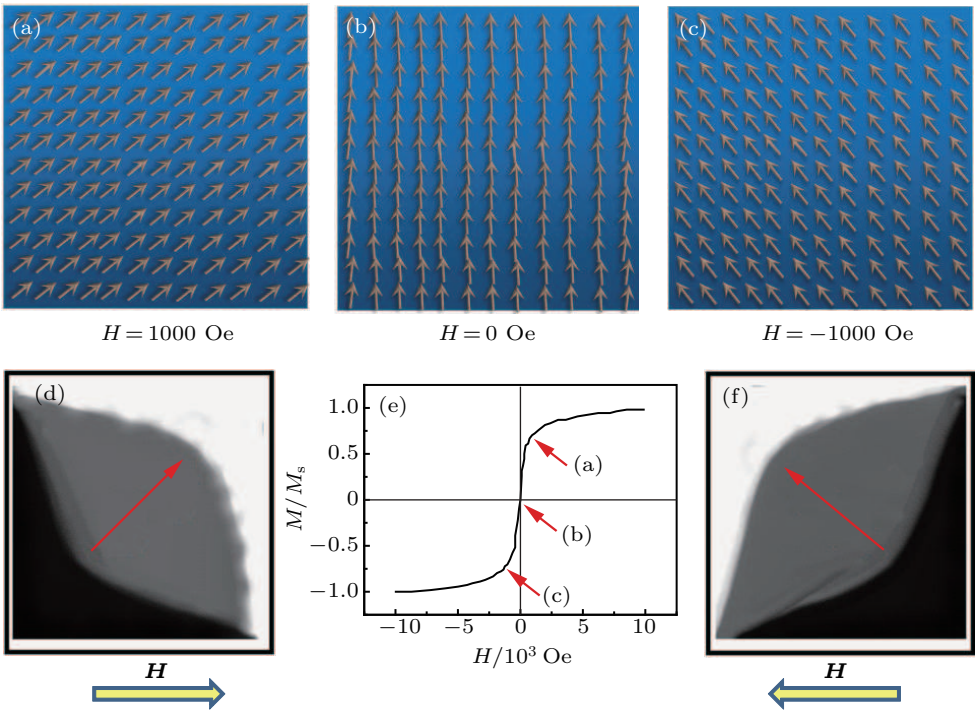


Fig. 4. Micromagnetic calculations. (a)–(c) Distribution of the spin configurations for the three situations highlighted by red arrows in the calculated hysteresis loop in (e). Panels (d) and (f) show the calculated MFM contrasts for the configurations shown in (a) and (c), respectively. (e) Calculated hysteresis loop for a single Fe_3O_4 nanoparticle.

4. Conclusion

In summary, the local detection of magnetic domains of isolated 10 nm-sized Fe_3O_4 MNPs has been investigated with field-variable MFM. The field-variable magnetic domain structures and magnetization process of Fe_3O_4 MNPs were determined locally in the nanometer scale with high spatial resolution. The present results suggest that the field-variable frequency-modulated MFM indeed provides a means to characterize the magnetization behaviors of individual MNPs with very small coercive force, thus enabling us to separately estimate the distributions of the dipolar fields and the local switching fields of the MNPs. Therefore, this technique has great potential to provide information on magnetic features of magnetic nanostructures, such as nanoparticles, nanodots, skyrmions, and vortex, with high spatial resolution. Such information is crucial for the development and application of magnetic nanostructures and devices.

References

[1] Sukhov A and Berakdar J 2009 *Phys. Rev. Lett.* **102** 057204
[2] Balan A, Derlet P M, Rodrguez A F, Bansmann J, Yanes R, Nowak U, Kleibert A and Nolting F 2014 *Phys. Rev. Lett.* **112** 107201
[3] Li X, Li Z, Pan D, Yoshimura S and Saito H 2014 *Appl. Phys. Lett.* **104** 213106
[4] Li X, Lu W, Song Y, Wang Y, Chen A, Yan B, Yoshimura S and Saito H 2016 *Sci. Rep.* **6** 22467
[5] Tudisco C, Bertani F, Cambria M T, Sinatra F, Fantechi E, Innocenti C, Sangregorio C, Dalcanale E and Condorelli G 2013 *Nanoscale* **5** 11438
[6] Zhu J, Lu Y J, Li Y G, Jiang J, Cheng L, Liu Z, Guo L, Pan Y and Gu H W 2014 *Nanoscale* **6** 199
[7] Brambilla D, Droumaguet B L, Nicolas J, Hashemi S H, Wu L P, Moghimi S M, Couvreur P and Andrieux K 2011 *Nanomedicine* **7** 521
[8] Yang C L, Rait A, Pirollo K F, Dagata J A, Farkas N and Chang E H 2008 *Nanomedicine* **4** 318
[9] López-Ortega A, Estrader M, Salazar-Alvarez G, Roca A G and Nogues J 2015 *Phys. Rep.* **553** 1
[10] Sun S N, Wei C, Zhu Z Z, Hou Y L, Subbu S V and Xu Z C 2014 *Chin. Phys. B.* **23** 037503
[11] Neumann A, Thonniben C, Frauen A, Hebe S, Meyer A and Oepen H P 2013 *Nano Lett.* **13** 2199
[12] Thirion C, Wernsdorfer W and Mailly D 2003 *Nat. Mater.* **2** 524
[13] Koelle D 2013 *Nat. Nanotechnol.8* **617**
[14] Wachowiak A, Wiebe J, Bode M, Pietzsch O, Morgenstern M and Wiesendanger R 2002 *Science* **298** 577
[15] Fischer P, Im M Y, Kasai S, Yamada K, Ono T and Thiaville A 2011 *Phys. Rev. B* **83** 212402
[16] Rondin L, Tetienne J P, Rohart S, Thiaville A, Hingant T, Spinicelli P, Roach J F and Jacques V 2013 *Nat. Commun.* **4** 2279
[17] Freeman M R and Choi B C 2001 *Science* **294** 1484
[18] Li Z and Li X 2014 *Acta Phys. Sin.* **63** 178503 (in Chinese)
[19] Hai G T, Zhao W X, Chen J S, Li Z H and He J L 2018 *Chin. Phys. Lett.* **35**
[20] Block S, Glöckl G, Weitschies W and Helm C A 2011 *Nano Lett.* **11** 3587
[21] Nocera T M , Chen J, Murray C B and Agarwal G 2012 *Nanotechnology* **23** 495704
[22] Schreiber S, Savla M, Pelekhov D V, Iscru D F, Selcu C, Hammel P C and Agarwal G 2008 *Small* **4** 270
[23] Sievers S, Braun K F, Eberbeck D, Gustafsson S, Olsson E, Schumacher H W and Siegner U 2012 *Small* **8** 2675
[24] Kim D, Chung N K, Allen S, Tendler S J B and Park J W 2012 *ACS Nano* **6** 241
[25] Moya C, Iglesias-Freire O, Pérez N, Batlle X, Labarta A and Asenjo A 2015 *Nanoscale* **7** 8110
[26] Pinilla-Cienfuegos E, Manas-Valero S, Forment-Aliaga A and Coronado E 2016 *ACS Nano* **10** 1764
[27] Sorop T G, Untiedt C, Luis F, Kroll M, Rasa M and Jongh L J 2003 *Phys. Rev. B* **67** 014402
[28] Ross C A et al 2002 *Phys. Rev. B* **65** 144417
[29] Ferre R and Ounadjela K 1997 *Phys. Rev. B* **56** 14066
[30] Margaris G, Trohidou K N, Iannotti V, Ausanio G, Lanotte L and Fiorani D 2012 *Phys. Rev. B* **86** 214425
[31] Lu W, Li Z, Hatakeyama K, Egawa G, Yoshimura S and Saito H 2010 *Appl. Phys. Lett.* **96** 143104